Proceedings of the 2006 IASME/WSEAS International Conference on Continuum Mechanics, Chalkida, Greece, May 11-13, 2006 (pp136-141)

Pattern Formation and Thermal Convection of Newtonian and Viscoelastic Fluids

ROGER E KHAYAT
Department of Mechanical and Materials Engineering
University of Western Ontario
London, Ontario
CANADA N5X 3R6

Abstract: - The influence of inertia and elasticity on the onset and stability of 3-D thermal convection is examined for highly elastic polymeric solutions with constant viscosity. These solutions are known as Boger fluids, and their rheology is approximated by the Oldroyd-B constitutive equation. The onset and the stability of steady convective patterns, namely rolls, hexagons and squares, are studied in the post-critical range of the Rayleigh number by using an amplitude equation approach. The square pattern is found to be unstable. In contrast to Newtonian fluids, the hexagonal pattern can be stable for a certain range of elasticity.

Key-Words: - Pattern formation, viscoelastic fluid, thermal convection.

1 Introduction

While the problem of Rayleigh-Bénard (RB) thermal convection has been extensively investigated for Newtonian fluids [1], relatively little attention has been devoted to the thermal convection of viscoelastic fluids. Flow instability and turbulence are far less widespread in viscoelastic fluids than in Newtonian fluids because of the high viscosity of polymeric fluids. Green [2], Vest & Arpaci [3], and Sokolov & Tanner [4] were the first to conduct the linear stability analysis of RB convection of an upper-convected Maxwell fluid. Nonlinear RB convection of non-Newtonian fluids was considered by Eltayeb [5], Rosenblatt [6], Martinez-Mardones & Pérez-Garçia [7], Harder [8], and Park & Lee [9]. Weakly nonlinear analyses were conducted by Martinez-Mardones et al [10], and Parmentier, Lebon & Regnier [11]. Khayat developed a low-order dynamical system approach to study the effect of elasticity on thermal convection [12]-[15]. More recently, Li and Khayat examined more accurately pattern formation for weakly nonlinear flow [16].

Some of the earlier experiments on the thermal convection of non-Newtonian fluids were conducted by Liang & Acrivos [17]. Their study, however, focused on the effects of shear thinning, which were found to enhance regularity in flow pattern. Kolodner [18] reported on and referred to recent experiments on the elastic behaviour of individual, long strands of DNA in buffer solutions, which seem to indicate the convective patterns take the form of spatially-localized standing and traveling waves that exhibit small amplitude and extremely long oscillation periods. The critical Rayleigh number for the onset of overstability is lower than for a Newtonian fluid, which is in agreement with linear stability analysis of viscoelastic fluids. Although both experimen[t] and theory indicate that two-dimensional rolls are favored at the onset of oscillatory or stationary convection, the emergence of three-dimensional patterns can be important. The prevalence of two-dimensional rolls, similarly to Newtonian flow, should be expected only near the onset, where the velocity gradients and therefore normal stresses are weak.

The linear stability analysis predicts the threshold for the onset of stationary or oscillatory RB convection. Once the instability threshold is obtained, the amplitude of the motion, the preferred pattern, the size of convective cells, and whether the nonlinear RB convection are unique or not can only be found via nonlinear analysis. The objective of the present study is to investigate the onset and stability of flow patterns in viscoelastic RB convection. A weakly nonlinear approach, amplitude equation method, is adopted. Details of the formulation and solution procedure are given by Li & Khayat [19]. The solutions of temperature, velocity, and stress components are expressed as series expansions in terms of the eigenfunctions of the linearized problem. These expansions are then substituted into the nonlinear equations and projected onto the eigenfunctions of the linear adjoint problem. This procedure results in an infinite set of ordinary differential equations that are then truncated by considering only a few sets of eigenfunctions.

2 Problem Formulation

Consider an incompressible fluid confined between two infinite and flat plates at $Z=-D/2$ and $Z=D/2$. Let T_0 and $T_0+\delta T$ be the temperatures of the upper and lower plates, respectively, with T_0 being the reference temperature and δT being the temperature difference. In the present study, the fluid is assumed to obey the following equation of state:

$$\rho(T)=\rho_0\left[1-\alpha_T(T-T_0)\right], \tag{1}$$

where ρ and ρ_0 are the densities at the temperatures T and T_0, respectively, and α_T is the coefficient of volumetric expansion. Let D, D^2/κ, κ/D, $\rho_0\kappa^2/D^2$, be, respectively, typical length, time, velocity and pressure, and $\eta\kappa/D^2$ be the typical stress. Here κ is the thermal diffusivity and η is the fluid viscosity. If the Boussinesq's approximation[i] is assumed to hold, then the dimensionless equations for the conservation of mass, momentum and energy, read, respectively:

$$\nabla\cdot u=0 \tag{2}$$

$$\mathrm{Pr}^{-1}\left(\mathbf{u}_{,t}+\mathbf{u}\cdot\nabla\mathbf{u}\right)=-\nabla p+\theta\mathbf{e}_z+\frac{Rv}{Rv+1}\Delta\mathbf{u}+\nabla\cdot\boldsymbol{\tau} \tag{3}$$

$$\theta_{,t}+\mathbf{u}\cdot\nabla\theta=\Delta\theta+\mathrm{Ra}\,\mathbf{u}\cdot\mathbf{e}_z \tag{4}$$

where ∇ is the gradient operator, and $\Delta=\nabla\cdot\nabla$ is the Laplacian operator. A subscript after a comma denotes partial differentiation. t is the time, $u=(u,v,w)$ is the velocity vector, p is the pressure deviation from the steady state, and $\mathbf{e}_z$ is the unit vector in direction opposite to gravity. $\theta=\frac{g\alpha_T D^3(T-T_s)}{\nu\kappa}$ is the departure from the steady-state temperature, $T_s=T_0-(Z/D-1/2)\delta T$, where g is the acceleration due to gravity, and $\nu=\eta/\rho_0$ is the kinematic viscosity. In this work, the fluids examined are highly elastic polymeric solutions with constant viscosity, η, and a single relaxation time, λ. These solutions are known as Boger fluids, and their rheology is approximated by the Oldroyd-B constitutive equation. The elastic part of the deviatoric stress tensor, $\boldsymbol{\tau}$, is given by [20]

$$E\left[\boldsymbol{\tau}_{,t}+\mathbf{u}\cdot\nabla\boldsymbol{\tau}-(\nabla\mathbf{u})^T\cdot\boldsymbol{\tau}-\boldsymbol{\tau}\cdot\nabla\mathbf{u}\right]=-\boldsymbol{\tau}+\frac{1}{Rv+1}\left[\nabla\mathbf{u}+(\nabla\mathbf{u})^T\right], \tag{5}$$

where a superscript T denotes matrix transposition. There are four important dimensionless parameters in the problem, namely the Rayleigh number, Ra, the Prandtl number, Pr, the elasticity number, E, and the solvent-to-solute viscosity ratio, Rv:

$$\mathrm{Ra}=\frac{\delta T g\alpha_T D^3}{\nu\kappa},\qquad \mathrm{Pr}=\frac{\nu}{\kappa},\qquad E=\frac{\lambda\kappa}{D^2},\qquad Rv=\frac{\eta_s}{\eta_p}. \tag{6}$$

In this study, the stress free boundary conditions at the plates are considered, which is given by

$$w=\theta=\frac{\partial^2 w}{\partial z^2}=0,\text{at } z=-1/2,1/2 \tag{7}$$

With the exception of density, the fluid parameters are assumed to be independent of temperature. In contrast to Taylor-Couette flow, the influence of temperature on rheological parameters, namely the relaxation time and viscosity, is not expected to be significant. The major influence of temperature for Taylor-Couette is of dissipative nature, which is bound to be significant given the relatively high critical Taylor or Deborah number at the onset of instability. Thermal convection of polymeric fluids can happen at relatively low temperature gradient or Rayleigh number. Chewing-gum solutions can boil at room temperature. More importantly, while the base state for Taylor-Couette flow is purely azimuthal flow, that for Rayleigh-Benard convection is pure heat conduction. Thus, the absence of flow in the base state makes the influence of dissipation, and therefore the temperature dependence of the rheological parameters, essentially negligible.

The solution of problem (1)-(7) is obtained by first carrying a linear stability analysis around the conductive state. In the postcritical range of Rayleigh number, the flow, temperature and stress fields are expanded in terms of the eigenfunctions of the linearaized flow. A Galerkin projection is carried out to obtain the equations that govern the expansion coefficients. These are of the Landau Ginsburg type [19].

3 Results and Discussion

For a small value of E or a large value of Rv, one expects the behaviour of the flow to be similar to the Newtonian regime, at least around the purely conductive state. Similarly to the case of a Newtonian fluid, one of the steady-state solution branches corresponds to pure heat conduction. As Ra exceeds a critical value, the conduction state loses its stability to steady convection. In contrast to Newtonian fluids, which admit only rolls in the post-critical range, viscoelastic convection can be in the form of rolls or hexagons depending on the level of elasticity (see below).

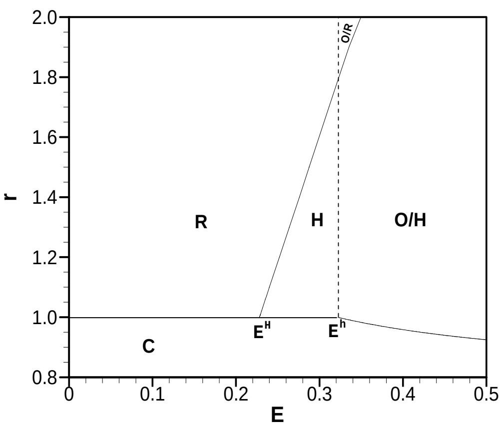

FIG. 1. Stability picture obtained with amplitude equation method for two convection patterns, namely roll and hexagon. This figure shows the stable range of roll and hexagonal patterns on (r,E) plane for a fluid with $\mathrm{Pr}=1000$ and $\mathrm{Rv}=3.75$. H and R represent stable regions for hexagonal and roll patterns, respectively, C the stable heat conduction state, and O the oscillatory convection. E^{H} represents the critical elasticity number for the emergence of three-dimensional convective pattern (hexagon), while E^{h} is the elasticity level corresponding to the onset of oscillatory convection.

Parmentier *et al.* [11] carried out a weakly nonlinear stability analysis of Bénard-Marangoni convection of viscoelastic fluids using an amplitude-equation method. Three cell patterns consisting of rolls, hexagons, and squares have been examined for stationary convection; oscillatory convection was not considered. The roll pattern was predicted to be stable for only small elasticity number ($\mathrm{E}<0.0035$) near criticality, and the three-dimensional hexagonal pattern was found to be stable for $\mathrm{E}\in[0.0035,0.07]$, for a fluid with $\mathrm{Pr}=1000$ and $\mathrm{Rv}\approx 0.01$. The square pattern was found to be always unstable (at least near criticality). It is observed that, according to the current linear stability analysis, the limit $\mathrm{E}=0.07$ corresponds to the critical elasticity number for the emergence of oscillatory thermal convection.

In this section, the amplitude equations are used to examine parameter ranges for three-dimensional stationary convection that have not been covered by Parmentier *et al.* [1] The stability of the steady rolls, hexagons and squares is determined through linear stability analysis of the steady state solutions of the amplitude equations [11] pertaining to each pattern. The current calculations are based on the free-free boundary conditions only, and indicate that the viscosity ratio has a strong influence on the stable ranges of stationary roll and hexagonal patterns. The square pattern is found to be always unstable. The stability picture is best illustrated in the (r,E) plane. Alternatively, the stability picture could be examined in the (r, De) plane, where De is the Deborah number. However, additional calculations (not included here) show that the De varies linearly with E, and, therefore no new qualitatively different insight would be gained. Fig. 1 shows typically the regions of existence of roll and hexagonal patterns for a fluid with $\mathrm{Rv}=3.75$ and $\mathrm{Pr}=1000$. In the figure, H and R denote stable hexagonal and roll regions, respectively. In contrast to the prediction of Parmentier *et al.* there is no region where both hexagon and roll patterns coexist, as a result of the use of different boundary conditions here. Despite this discrepancy, qualitative agreement is obtained regarding the stable ranges of hexagonal and roll patterns. For relatively small E, the conductive state, C, is lost to two-dimensional stationary convection (rolls) when r exceeds unity. When the level of elasticity exceeds a critical value E^{H}, but remains smaller than E^{h} (elasticity level corresponding to the onset of oscillatory convection), only the hexagonal pattern is stable at the onset of stationary convection. Beyond E^{h}, oscillatory convection sets in. Thus, inertia tends to enhance the onset of convective rolls. It is found that E^{H} increases linearly with r, which seems to be the case for other values of Rv and Pr. The figure also indicates that E^{H} can be larger than E^{h} at higher Rayleigh number, which means that both stationary roll and oscillatory convection become possible. This region is indicated by O/R in the figure. For $\mathrm{E}>\mathrm{E}^{\mathrm{h}}$, the conductive state loses its stability at $\mathrm{r}<1$ as predicted by linear stability analysis.

Similarly, there is a region marked by O/H, where both stationary hexagons and oscillatory convection are possible.

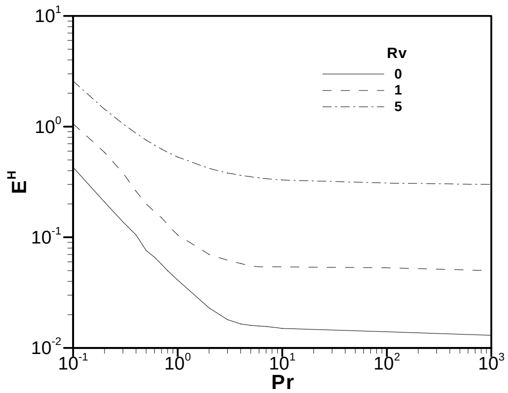

FIG.2. Influence of Pr on the critical elasticity number E^H for different value of Rv. The curves show that E^H decreases monotonically with Pr.

The dependence of E^H on the fluid parameters is summarized in Fig. 2 and 3, where E^H is plotted against Pr and Rv at $r = 1.1$, respectively. Fig. 2 shows the influence of Pr on E^H for $\mathrm{Rv} \in [0,5]$. Two distinct regimes can be discerned from Fig. 2.

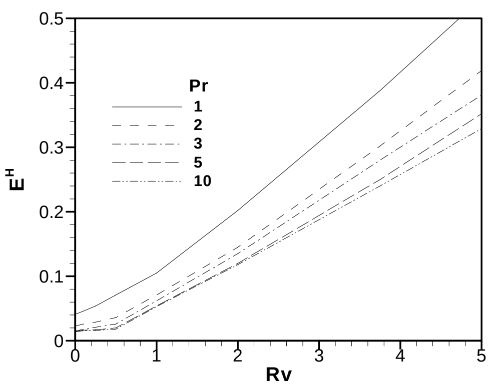

FIG. 3. Influence of Rv on the critical elasticity number E^H for different value of Pr. The curve show the linear dependence of E^H on Rv when $\mathrm{Rv} > 0.5$.

For small Pr values, E^H drops sharply like $\mathrm{Pr}^{0.93}$ regardless of the viscosity ratio. In this range, the roll pattern appears to be preferred unless E is relatively large. Thus, rarefied gases ($\mathrm{Pr} << 1$ and $\mathrm{Rv} = 0$) would exhibit a predominantly roll pattern. For larger Pr values, E^H remains essentially constant. The curves become flattened, which indicates that for typical polymeric solutions ($\mathrm{Pr} >> 1$), the influence of Pr on the stationary convective patterns is not significant. Thus, it is the viscosity ratio of the polymeric solution that determines the likelihood for two- or three-dimensional convection. Note that E^H tends to infinity, for any Pr, in the limit of a Newtonian fluid ($\mathrm{Rv} \to \infty$). This can be seen more clearly from Fig. 3, which shows the increase of E^H with Rv for several values of Pr. The increase is slow when Rv is relatively small. For large Rv, the figure indicates that E^H is simply proportion to Rv, and this behaviour may be given by

$$E^H \approx 0.07\mathrm{Rv} - 0.022, \qquad (\mathrm{Pr} >> 1) \qquad (8)$$

Thus, similarly to elasticity, viscosity tends to precipitate the emergence of three-dimensional convection, as well as the onset of oscillatory behaviour. There is thus a synergetic interplay between elastic and viscous effects regarding the loss of stability of the roll pattern. The stable range of two-dimensional roll pattern is significantly widened with increasing Rv, which is of course expected as the contribution of the Newtonian solvent increases. Recall, that in the Newtonian limit, only rolls are predicted, regardless of the nature of boundary conditions used[ii].

Unlike the critical Rayleigh number, Ra_C^S at the onset of stationary thermal convection, the amplitude of convection is strongly influenced by fluid elasticity, viscosity ratio, and Prandtl number. It is convenient to monitor the response of the Nusselt number, Nu, as Ra is increased in the post-critical range. The Nusselt number is defined in terms of the heat flux, Q, at the lower plate, averaged over a cell width:

$$\mathrm{Nu} = 1 - \frac{1}{\mathrm{Ra}} \left\langle \theta_{,z}\left(x, y, z = -1/2, t\right) \right\rangle$$

$$= 1 - \frac{1}{\mathrm{Ra}} \sum_p \sum_q A_q^p \Theta_q^p p\pi \cos\left(\frac{p\pi}{2}\right) \left\langle e^{ik_q\left(x\cdot\mathbf{e}_x + y\cdot\mathbf{e}_y\right)} \right\rangle \qquad (9)$$

where $\langle\ \rangle$ denotes double integration over $x \in [0, 2\pi/k]$ and $y \in [0, 2\pi/k]$.

The influence of fluid elasticity on the steady bifurcation picture of roll pattern is depicted in Fig. 4, where Nu is plotted against r for $E \in [0, 0.2]$, $\mathrm{Rv} = 3.75$, and $\mathrm{Pr} = 7$. E is chosen relatively small to insure that the exchange of stability between conductive state and stationary roll pattern is valid. The figure indicates that fluid elasticity tends to prohibit heat transport, relatively to a Newtonian fluid. The bifurcation is supercritical, reflecting a gradual increase in Nu as r exceeds slightly one.

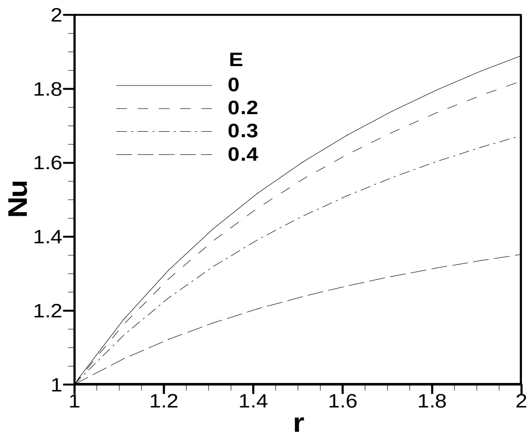

FIG.4. Bifurcation diagrams and influence of elasticity on stationary thermal convection of roll patterns. Nusselt number is plotted against the reduced Rayleigh number r for $\mathrm{E} \in [0, 0.2]$ with $\mathrm{Rv} = 3.75$ and $\mathrm{Pr} = 7$.

Near the critical point, the influence of E is gradual, with Nu decreasing almost linearly as E increases.

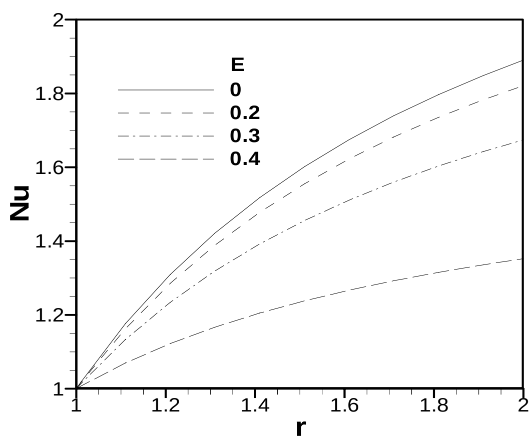

FIG.5. Bifurcation diagrams and influence of viscosity ratio on stationary thermal convection of hexagonal patterns. Nusselt number is plotted against the reduced Rayleigh number r for $\mathrm{E} \in [0.2, 0.4]$ with $\mathrm{Rv} = 3.75$ and $\mathrm{Pr} = 7$.

At higher r values, the drop in Nu between two successive E values is largest near $\mathrm{E} = 0$. Thus, elasticity appears to affect little the steady-state thermal convection for the higher Rayleigh number range. Physically, one expects the dependence of Nu on E to be continuous as the flow deviates from the Newtonian limit. At higher elasticity level, the conductive state loses its stability to stationary hexagonal convective pattern as r exceeds one. The steady bifurcation picture of hexagonal pattern is also supercritical as depicted in Fig. 5, the plot of Nu against r for $\mathrm{E} \in [0.2, 0.4]$, $\mathrm{Rv} = 3.75$, and $\mathrm{Pr} = 7$. The drop in Nu between two successive E values becomes larger as r increasing, which indicates that elasticity affects much the steady-state thermal convection for the higher Rayleigh number range. For $\mathrm{Rv} = 3.75$, elasticity tends to prohibit heat transport. However, this is not always the case. The heat transport is actually enhanced with increasing elasticity as depicted in Fig. 6, which is the plot of Nu against E for $\mathrm{Rv} \in [2, 6]$, $\mathrm{r} = 2$, and $\mathrm{Pr} = 10$.

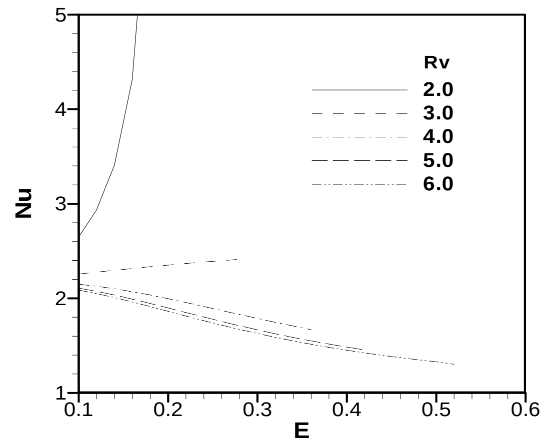

FIG.6. Influence of elasticity on stationary thermal convection of hexagonal pattern. Nusselt number is plotted against the elasticity number E for $\mathrm{r} = 2$ with $\mathrm{Rv} = 3.75$ and $\mathrm{Pr} = 7$.

The influence of viscosity ratio on Nusselt number for steady roll pattern is shown in Fig. 7, which parallels the influence of elasticity as Rv decreases. Recall that as the (Newtonian) solvent viscosity decreases, the effective elasticity of the fluid becomes more significant. Indeed, the figure indicates that Nu decreases with decreasing Rv for a given r. Fig. 4, 5, and 7 seem to suggest that there is little influence of fluid elasticity or relaxation on the amplitude of steady convection when r is close to one. This observation is in agreement with the measurements of Liang & Acrivos [17]. It is important to observe that the physical significance of the branch curves in Fig. 4, 5, and 7 become clear only when the stability of these branches is known. It is found that Prandtl number has less influence on the amplitude of both roll and hexagonal convective patterns. For fixed elasticity number and viscosity ratio, Nusselt number keeps essentially the same as Pr varies from 1 to

1000, as shown in Fig. 8, which is the plot of Nu for

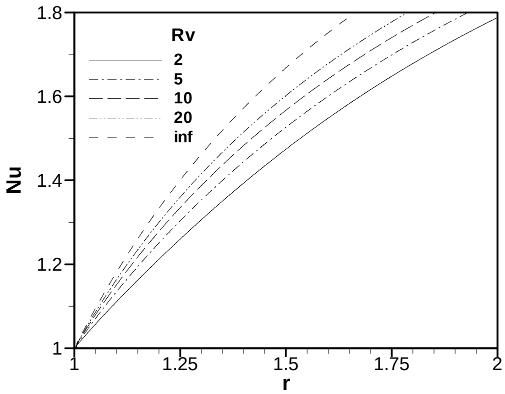

FIG. 7. Bifurcation diagrams and influence of viscosity ratio on stationary thermal convection of roll patterns. Nusselt number is plotted against the reduced Rayleigh number r for $\mathrm{Rv} \in [5, \infty]$ with $\mathrm{E} = 0.1$ and $\mathrm{Pr} = 7$.

steady hexagonal pattern against r for $\mathrm{E} = 0.3$ and $\mathrm{Rv} = 3.75$. The inset clearly shows an asymptotic behaviour.

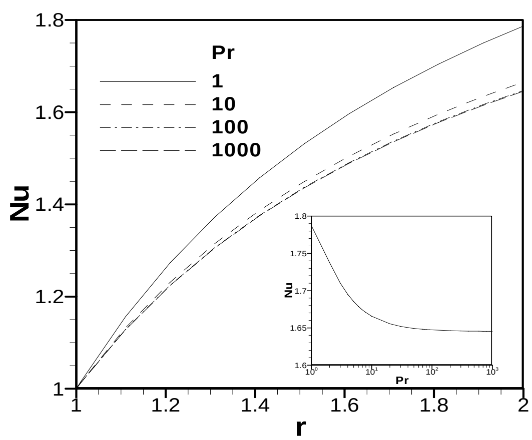

FIG.8. Bifurcation diagrams and influence of Pr on stationary thermal convection of hexagonal patterns. Nusselt number is plotted against the reduced Rayleigh number r for $\mathrm{Pr} \in [1, 1000]$ with $\mathrm{Rv} = 3.75$ and $\mathrm{E} = 0.3$. Inset shows the asymptotic behaviour of Nu against Pr.

4 Conclusion

The finite-amplitude thermal convection for a thin layer of a viscoelastic fluid of the Oldroyd-B type is examined in this study. An amplitude equation approach is used to study the stability of stationary convective patterns, namely rolls, hexagons and squares, in the post-critical range of the Rayleigh number.. Square patterns are found to be unstable for any parameter range. Steady hexagonal patterns are predicted to be stable for certain range of elasticity number, which is in contrast to the Newtonian case, where only rolls are predicted to be stable. The influence of the Prandtl number and the viscosity ratio on the stability of rolls and hexagons are examined. It is found that the viscosity ratio plays a more important role in determining the likelihood of the two- or three-dimensional patterns for typical polymeric solutions.

References:

[1] E. L. Koschmieder, *Bénard Cells and Taylor Vortices* (Cambridge University Press, New York, 1993)
[2] T. Green, Phys. Fluids 11, 1410 (1968).
[3] C. M. Vest and V. S. Arpaci, J. Fluid Mech. 36, 613 (1969).
[4] M. Sokolov and R. I. Tanner, Phys. Fluids 15, 534 (1972).
[5] I. A. Eltayeb, Proc. Roy. Soc. Lond. A356, 161 (1977).
[6] S. Rosenblat, J. Non-Newtonian Fluid Mech. 21, 201 (1986).
[7] J. Martínez-Mardones and C. Pérez-García, 11 Nuovo Cimento 14, 961 (1992).
[8] H. Harder, J. Non-Newtonian Fluid Mech. 36, 67 (1991).
[9] H. M. Park and H. S. Lee, J. Non-Newtonian Fluid Mech. 66, 1 (1996).
[10] J. Martínez-Mardones, R. Tienmann, D. Walgraef, and W. Zeller, Phys. Rev. E. 54, 1478 (1996).
[11] P. Parmentier, G. Lebon, and V. Regnier, J. Non-Newtonian Fluid Mech. 89, 63 (2000).
[12] R. E. Khayat, J. Non-Newtonian Fluid Mech. 53, 227 (1994).
[13] R. E. Khayat, J. Non-Newtonian Fluid Mech. 58, 331 (1995).
[14] R. E. Khayat, Phys. Rev. E 51, 380 (1995).
[15] R. E. Khayat, J. Non-Newtonian Fluid Mech. **63**, 153 (1996).
[16] Z. Li and R. E. Khayat, J. Fluid Mech. **529**, 221 (2005)
[17] S. F. Liang and A. Acrivos, Rheol. Acta **9**, 447 (1970).
[18] P. Kolodner, J. Non-Newtonian Fluid Mech. **75**, 167 (1998).
[19] Z. Li and R. E. Khayat, Phys. Rev. E **71**, 066305 (2005).
[20] R. B. Bird, R. C. Armstrong, and O. Hassage, *Dynamics of Polymeric Liquids*, edition (John Wiley & Sons, New York, 1987), Vol. **1**.